Cataloging High-Quality Two-Dimensional van der Waals Materials with Flat Bands

Jingyi Duan,[1, 2, 3, #] Da-Shuai Ma,[4, 1, 2, #] Run-Wu Zhang,[1, 2, †] Zeying Zhang,[5]
Chaoxi Cui,[1, 2] Wei Jiang,[1, 2] Zhi-Ming Yu,[1, 2] and Yugui Yao[1, 2, ‡]
1Centre for Quantum Physics, Key Laboratory of Advanced Optoelectronic Quantum Architecture and Measurement (MOE),
School of Physics, Beijing Institute of Technology, Beijing 100081, China

Abstract

More is left to do in the field of flat bands besides the known research efforts. One of these unexplored areas is the flat bands featured in the two-dimensional (2D) van der Waals (vdW) materials. Compared to 3D crystals, the 2D vdW materials with a lower dimension could easily map out prominent flat-band lattice models and provide more straightforward visual evidence for the capture of prime features. Since vdW materials are potentially applicable to the study of flat-band physics, it is urgent to develop a simple and efficient approach to finding realistic vdW crystals with desired flat bands. Here, we utilize a powerful high-throughput tool to screen feasible vdW materials based on the Inorganic Crystal Structure Database. Through layers of filtration, we obtained 861 potential monolayers from 187093 items. Unlike existing screening schemes, a simple, universal rule, i.e., 2D flat-band score criterion, is first proposed to efficiently identify 229 flat-band candidates, and guidance is provided to diagnose the quality of flat bands in 2D systems. From the experimental accessibility perspective, we further provide a sub-catalog of 74 high-quality flat-band candidates among those selected 229 flat-band materials. All these efforts to screen experimental available flat-band candidates will certainly motivate continuing exploration toward the realization of this class of special materials and their applications in material science.

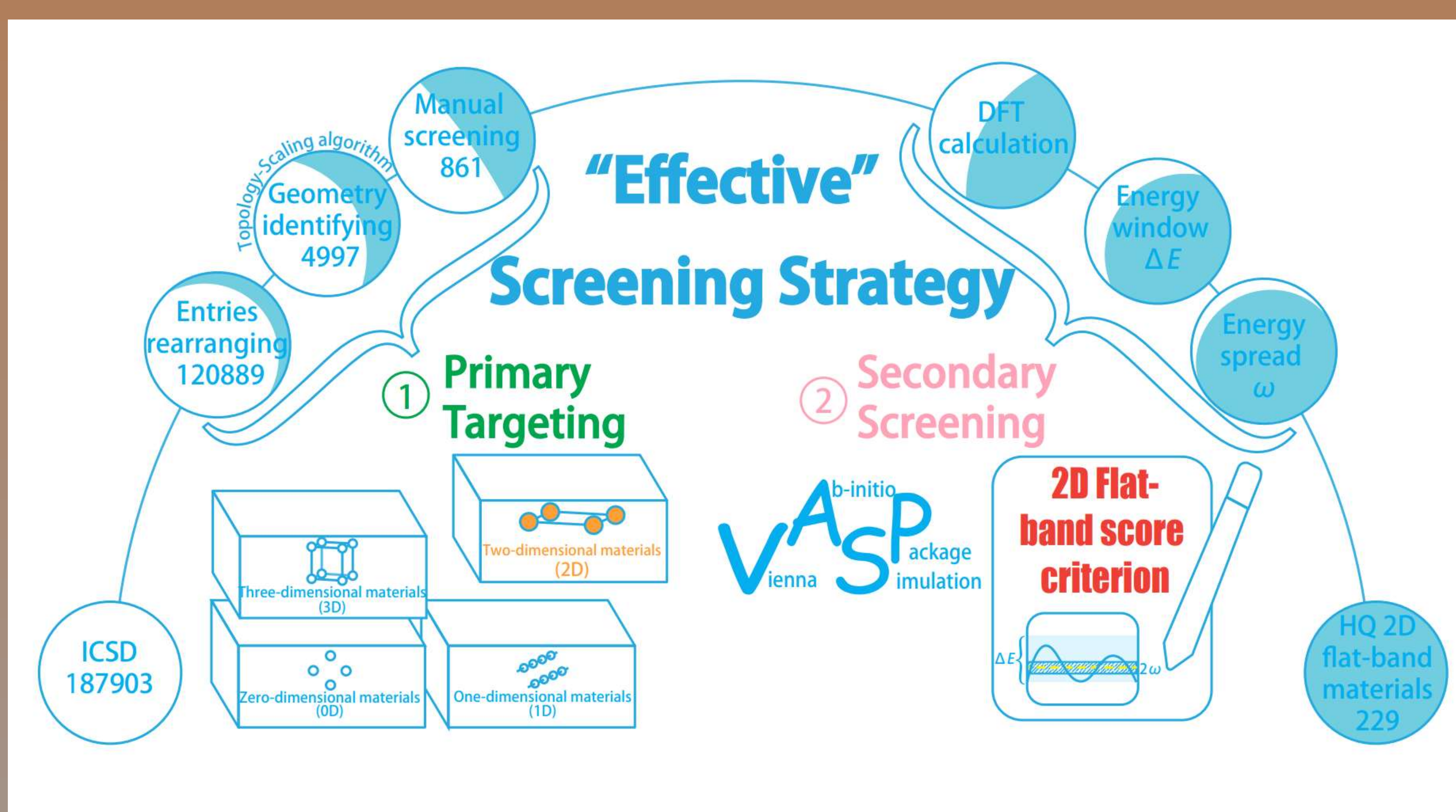

Figure 1. The schematic flowchart of screening 2D van der Waals flat-band materials. This workflow can identify the features of flat bands and illustrate the details of constructing a high-quality *Flat-band Materials Category* by two tiers: *primary targeting* and *secondary screening*.

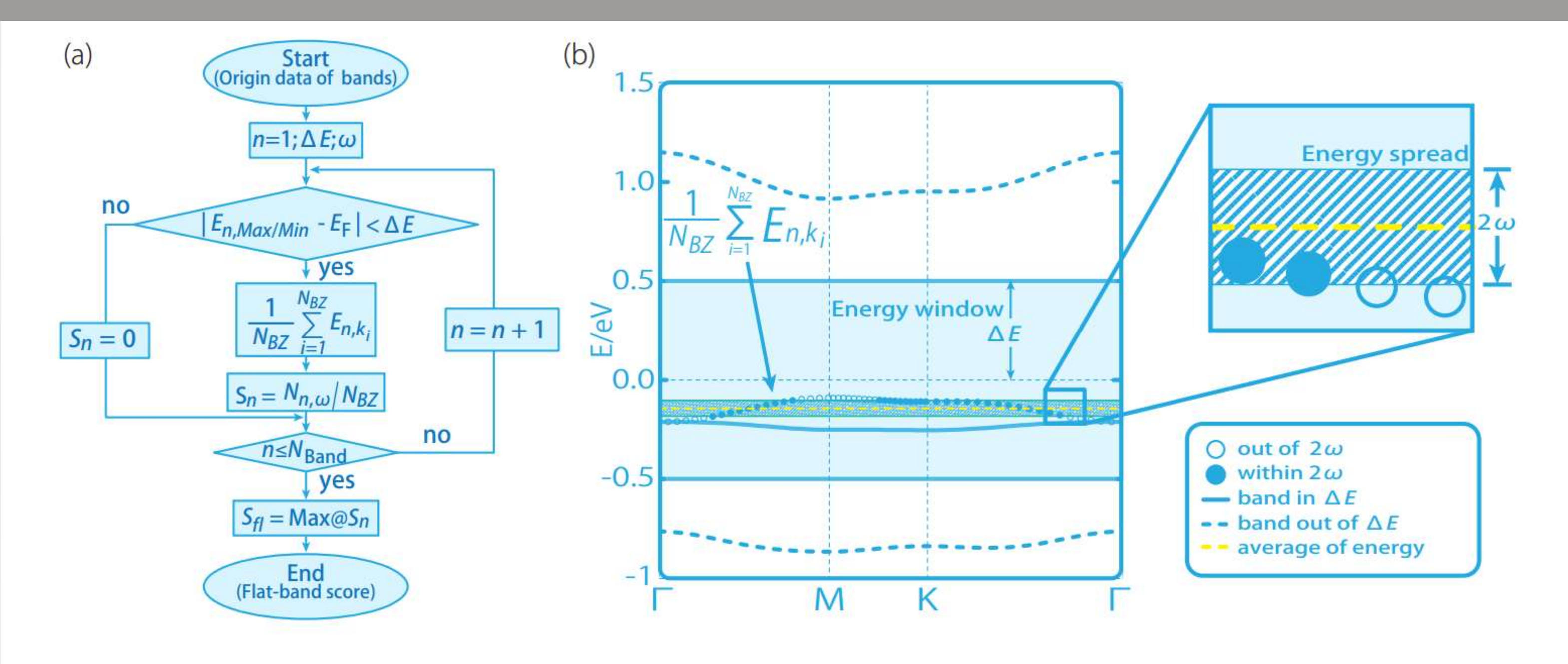

Figure 2. (a) Workflow to construct the 2D flat-band score criterion; the core part is to determine the energy window ΔE and the energy spread ω. (b) Graphical representation of the algorithm for numerically defining the flatness of band structure. Here we show the evaluation process when $\Delta E = 0.5$ eV and $\omega = 25$ meV. The light blue area represents the area covered by the energy window ΔE, and only the band that is wholly located in the energy window ΔE is scored separately. The yellow dashed line represents the average value of the energy of the band plotted in blue solid dots and blue hollow dots, and the blue and white diagonal striped area represents the effective area defined by the expansion of the yellow dashed line along with the $\pm\omega$.

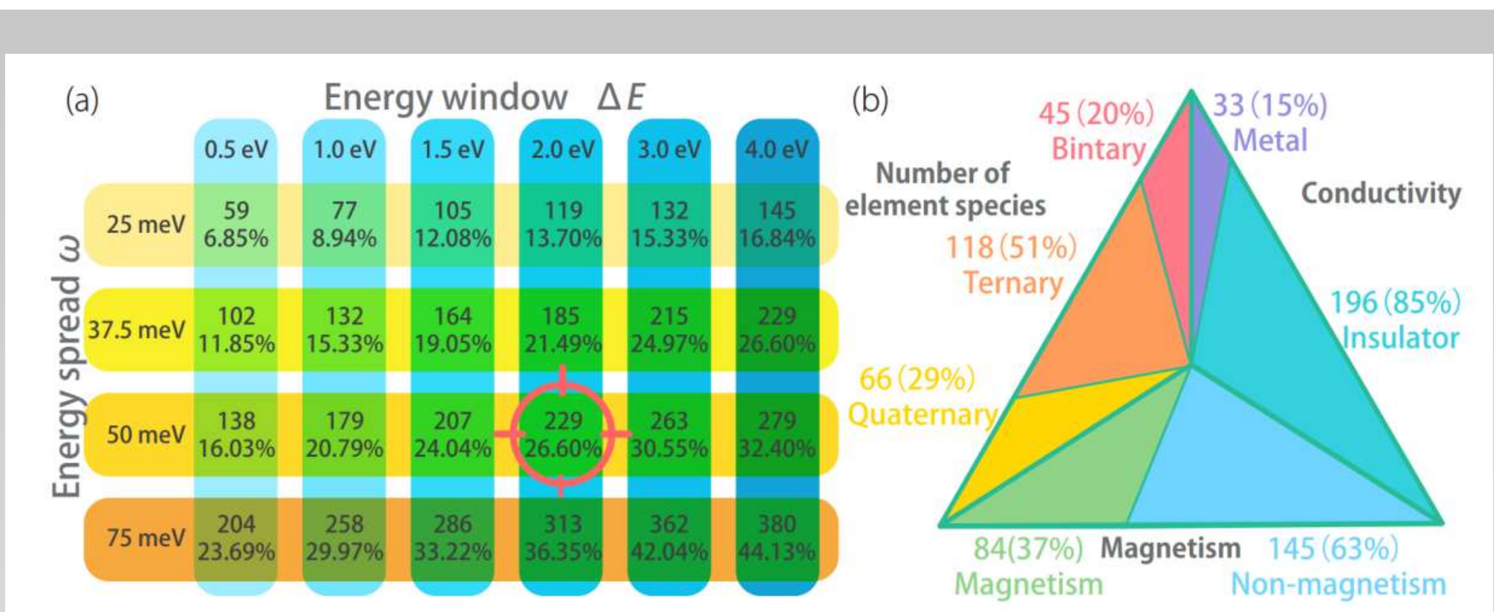

Figure 3. (a) Distribution of high-quality flat-band materials discrete values of ω and ΔE. (b) Classification of fingerprint characteristics of 229 flat-band materials obtained by $\omega = 50$ meV and $\Delta E = 2$ eV, including the number of element species, conductivity, and magnetism.

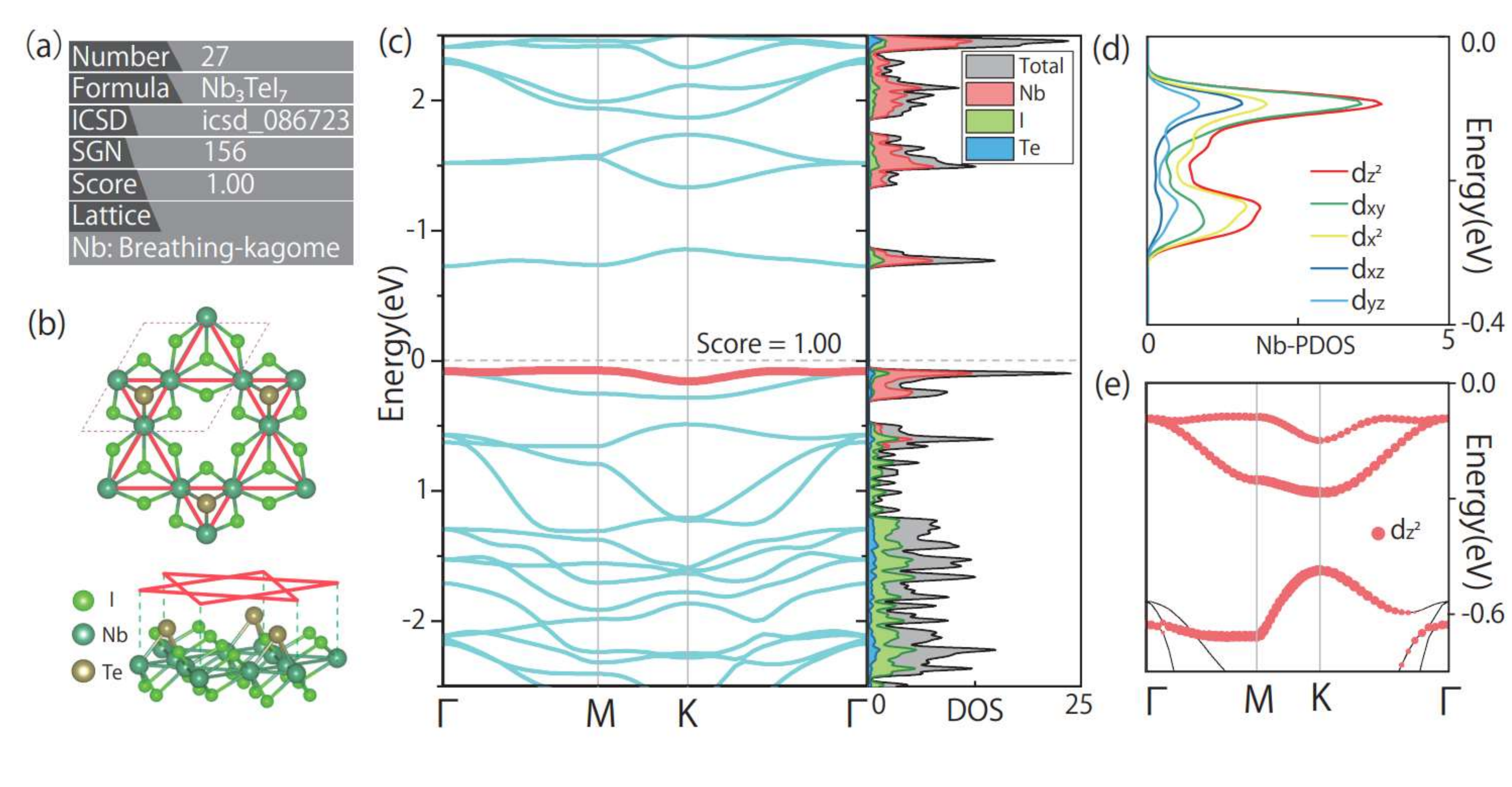

Figure 4. Geometric structure and band structure of the representative flat-band material Nb_3TeI_7. (a) Statistics of the candidate's entries include serial number, chemical formula, ICSD number of corresponding 3D material, space group number (SGN), and flat-band score (Score). The crystal structures of Nb_3TeI_7 (b), feature an apparent breathing-kagome lattice formed by the Nb atoms (in red). The band structure and density of states of the flat-band characterization for Nb_3TeI_7 are plotted in (c). In the band-structure plots, a flat band is remarked by the solid red line and is labeled score=1.00. The orbital characters of the colored bands are provided in (d) and (e)

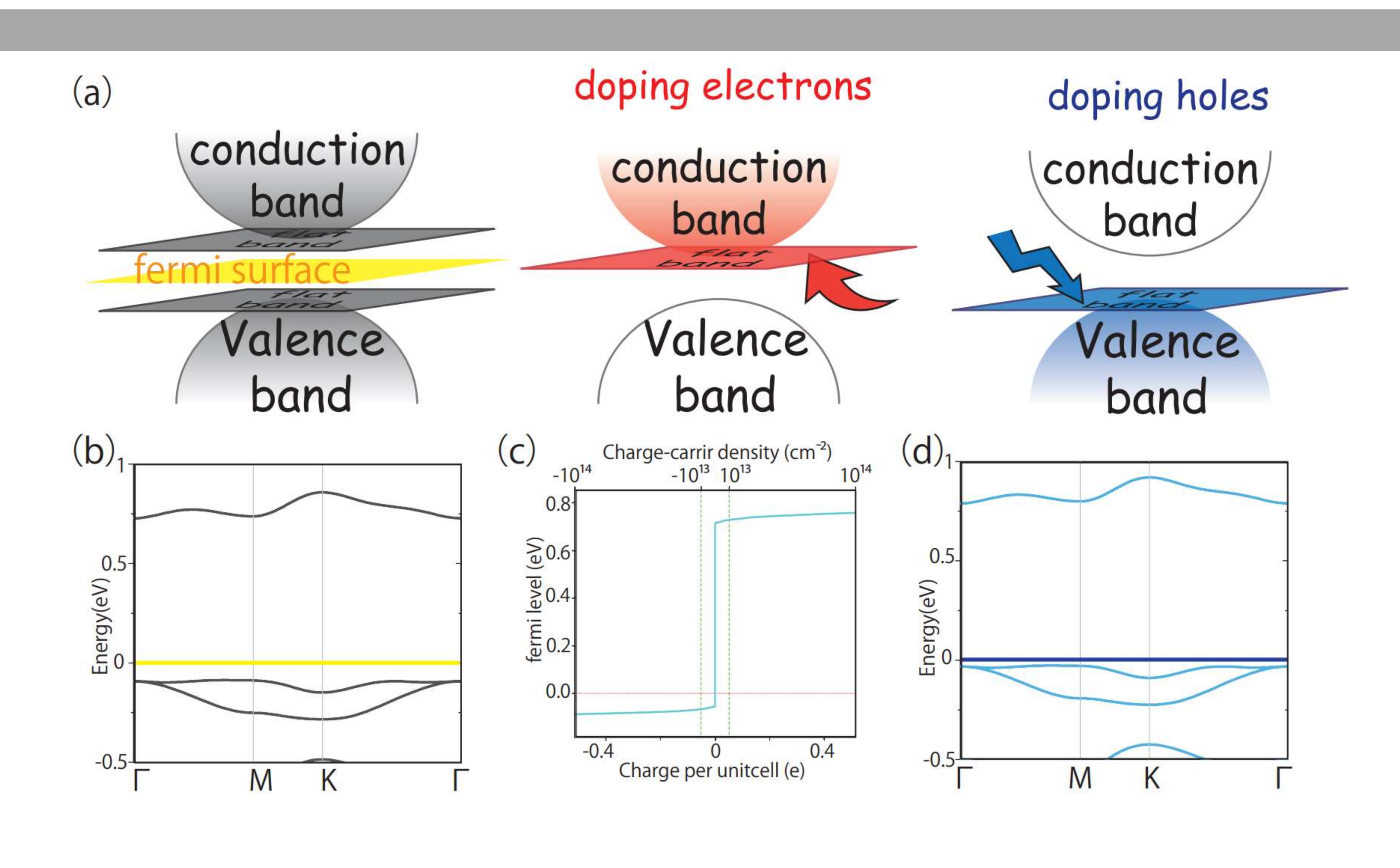

Figure 5. (a) A schematic illustration of transforming a potential flat-band material into a high quality flat-band material by adjusting the flat-band position to the Fermi level by doping. The electronic structures of undoped (b) and doped (d) Nb_3TeI_7. (c) The hole-doping charge as a function of the Fermi energy.

In this work, we have performed a systematic search for flat-band vdW materials and, we found that 229 items (score criterion: ω = 50 further explored the flat-band physical mechanism by mapping the types of lattices from the vdW candidates. By implementing effective screening strategies for 861 unique monolayers and ΔE = 2 eV) host high-quality flat bands. From the standpoint of experimental feasibility, we provide a sub-catalog of 74 high-quality flat-band candidates among those selected 229 flat-band materials. Our results work as a guide for future theoretical and experimental studies on 2D flat-band vdW materials where exotic physics phenomena such as magnetism and superconductivity can be further explored.

arXiv preprint arXiv:2204.00810 (2022).